Attempts to prepare the 17-electron (η^5-C_5H_5)MoX_2(dmpe) (X = Cl, Br, I; dmpe = bis(dimethylphosphino)ethane) compounds. Formation and X-ray molecular structure of (η^5-C_5H_5)$MoCl_3$(dmpe) and [(η^5-C_5H_5)-$Mo(dmpe)_2$][$MoBr_4$(dppe)] (dppe = bis(diphenylphosphino)ethane)

Beth E. Owens and **Rinaldo Poli***

Department of Chemistry and Biochemistry, University of Maryland, College Park, MD 20742 (U.S.A.)

(Received August 1, 1990)

Abstract

The reaction of $[Cp_2Mo_2Cl_5]^-$ with dmpe, followed by work-up in CH_2Cl_2 produced $CpMoCl_3$(dmpe). From the reaction of $CpMoBr_2$(dppe) (Cp = η^5-C_5H_5) with dmpe the salt [CpMo(dmpe)$_2$][$MoBr_4$(dppe)] was isolated. Crystal data: $CpMoCl_3$(dmpe): monoclinic, space group $P2_1/n$, $a = 8.1763(6)$, $b = 13.643(1)$, $c = 14.948(2)$ Å, $\beta = 103.054(8)°$, $V = 1624.3(6)$ Å^3, $Z = 4$, $D_c = 1.71$ g cm^{-3}, $R = 0.046$, $R_w = 0.070$ for 155 parameters and 1876 observations with $F_o^2 > 3\sigma(F_o^2)$; [CpMo(dmpe)$_2$][$MoBr_4$(dppe)]: monoclinic, space group $P2_1/n$, $a = 17.642(4)$, $b = 29.040(4)$, $c = 19.721(3)$ Å, $\beta = 99.28(1)°$, $V = 9972(5)$ Å^3, $Z = 8$, $D_c = 1.70$ g cm^{-3}, $R = 0.100$, $R_w = 0.119$ for 651 parameters and 3976 observations with $F_o^2 > 2.5\sigma(F_o^2)$.

Introduction

We are currently studying 17-electron compounds of Mo(III) of formula $CpMoX_2L_2$ and $CpMoX_2$(L-L) (X = Cl, Br, I; L = monodentate phosphine, L-L = bidentate phosphine) [1, 2]. These complexes exhibit a low spin ($S = 1/2$) electronic configuration, display significant Mo–P π and Mo–Cp δ backdonation, are oxidized easily and reversibly to the corresponding Mo(IV) 16-electron cations, and display dissociative ligand exchange kinetics [3].

During the investigations of compounds with chelating phosphine ligands, we have prepared the mononuclear $CpMoX_2$(dppe) compounds (X = Cl, Br, I) [2]. We report here our attempts to prepare analogous derivatives with dmpe as the bidentate ligand. The monomeric $CpMoX_2$(dmpe) molecules were formed as transient species, but these were unstable and decomposed as shown by EPR spectroscopy. The compounds $CpMoCl_3$(dmpe) and [CpMo(dmpe)$_2$]-[$MoBr_4$(dppe)], whose structures are reported here, were obtained as decomposition products in different reaction conditions.

Experimental

All operations were carried out under an atmosphere of dinitrogen. Solvents were dehydrated by conventional methods and distilled under dinitrogen prior to use. The EPR spectra were recorded on a Brucker ER200 instrument. The UV–Vis spectra were recorded at room temperature in CH_2Cl_2 as solvent on a Schimadzu UV-240 instrument. The FT-IR spectra were recorded on a Nicolet 5DXC spectrophotometer. The $MoX_3(THF)_3$ (X = Cl [4], Br [5], I [6]), MoX_3(dppe)(THF) (X = Cl, Br, I) [5] and $CpMoCl_4$ [2] starting materials were prepared as described in the literature. The ligands dppe and dmpe were purchased from Strem and used without further purification.

Preparation of $CpMoCl_3$(dmpe)

A total of 0.353 g of $CpMoCl_4$ (1.17 mmol) was reduced with two equivalents of amalgamated (1%) sodium. After filtration through Celite, the resulting brown solution of $[Cp_2Mo_2Cl_5]^-$ [7] was treated with dmpe (215 μl, 1.43 mmol). The solution immediately lightened to a light brown with production of a flocculent tan precipitate. The prompt recording of an EPR spectrum on the supernatant liquid showed a binomial quintet at $g = 1.988$ ($a_p = 20.4$ G). The mixture was stirred at room temperature for two days, after which period the solution was EPR silent. After evaporation to dryness at reduced pressure, the residue was extracted with CH_2Cl_2 affording a purple solution and a dark brown precipitate. After filtration, crystals of $CpMoCl_3$(dmpe) (0.053 g, 11%)

*Author to whom correspondence should be addressed.

0020-1693/91/$3.50

were obtained by diffusion of toluene. *Anal.* Calc. for $C_{11}H_{21}Cl_3MoP_2$:C, 31.64; H, 5.07; Cl, 25.47; P, 14.82. Found: C, 31.85; H, 5.00; Cl, 25.04; P, 15.78%. ^1H NMR (δ, CD_2Cl_2): 5.08 (dd, Cp, 5H, $J_1=0.77$ Hz, $J_2=2.89$ Hz), 2.45–2.15 (m, $Me_2PCH_2CH_2PMe_2$, 4H), 1.78 (d, PMe_2, 6H, $J=11.83$ Hz), 1.44 (d, PMe_2, 6H, $J=9.85$ Hz). $^{31}P\{^1H\}$ NMR (δ, CD_2Cl_2): 52.5 (d, $J=53.7$ Hz), 46.6 (d, $J=53.7$ Hz). A single crystal for the X-ray analysis was obtained from CH_2Cl_2/heptane.

Preparation of [CpMo(dmpe)$_2$][MoBr$_4$(dppe)]

$MoBr_3(THF)_3$ (0.754 g, 1.87 mmol) and dppe (0.547 g, 1.37 mmol) were placed in 75 ml of THF producing a red–orange suspension. When the dissolution of the solid was complete (*c.* 5h) TlCp (0.369 g, 1.37 mmol) was added producing a darker red–brown solution with immediate formation of a tan precipitate. After stirring at room temperature for *c.* 17 h, the deep orange solution was filtered through Celite and left to stand for three days. No significant decomposition of the $CpMoBr_2$(dppe) product (as monitored by EPR) was observed during this period of time. At this point the solution was refiltered to eliminate minor amounts of a solid which had formed, and dmpe (230 μl, 1.38 mmol) was added. A fine light orange precipitate formed over the period of several hours, while the color of the solution turned pale orange. After filtering off this solid (0.318 g), the solution was allowed to stand at room temperature for 5 days to produce two types of crystals — large orange needles and small reddish purple cubes — along with a white powder. The mother liquor was decanted off and the crystals were washed with THF and dried under vacuum (22 mg). The orange needles became opaque during the vacuum treatment, probably because of the loss of solvent of crystallization. They dissolved in CH_2Cl_2 to produce an EPR silent solution. The purple cubes were investigated crystallographically (*vide infra*). They are only sparingly soluble in CH_2Cl_2 to produce EPR silent solutions. The UV–Vis spectrum showed bands (in decreasing order of intensity) at 322, 368 and 442 nm. IR (Nujol mull, cm^{-1}): 3070m, 3050s, 1585w, 1570m, 1485s, 1435vs, 1420s, 1365s, 1340w, 1300m, 1285s, 1235vw, 1190m, 1160w, 1145vw, 1130w, 1095s, 1070m, 1030m, 1000m, 935vs, 910s, 895s, 870m, 830m, 825m, 815m, 800m, 765m, 755s, 710vs, 700vs, 665vw, 660vw, 650vw, 630s, 520vs, 500vs, 470m, 455w, 420w.

X-ray crystallography

CpMoCl$_3$(dmpe)

A single crystal was covered with a protective layer of epoxy cement, glued on the tip of a glass fiber, and mounted on the diffractometer. Crystal data are reported in Table 1. The cell determination, data collection and reduction and absorption correction [8a] were carried out in a routine manner. The structure was solved by direct methods and refined by alternate cycles of full-matrix least-square refinements and difference Fourier maps. The hydrogen atoms were introduced at calculated positions and used for structure factor calculations but not refined. The dmpe carbon atoms showed high thermal activity, which is consistent with the knowledge that dmpe ligands undergo a facile 'twisting' among the two limiting twisted conformations in crystal structures. Final atomic coordinates and equivalent isotropic thermal parameters are listed in Table 2, and selected bond distances and angles are in Table 3.

TABLE 1. Crystal data

Compound	$CpMoCl_3$(dmpe)	[CpMo(dmpe)$_2$][MoBr$_4$(dppe)]
Formula	$C_{11}H_{21}Cl_3MoP_2$	$C_{43}H_{61}Br_4Mo_2P_6$
Formula weight	417.53	1275.29
Space group	$P2_1/n$	$P2_1/n$
a (Å)	8.1763(6)	17.642(4)
b (Å)	13.643(1)	29.041(4)
c (Å)	14.948(2)	19.721(3)
β (°)	103.054(8)	99.28(1)
V (Å^3)	1624.3(6)	9972(5)
Z	4	8
D_{calc} (g cm^{-3})	1.71	1.70
μ(Cu Kα) (cm^{-1})	130.94	105.35
Radiation (monochromated in incident beam)	Cu Kα ($\lambda=1.54178$ Å)	Cu Kα ($\lambda=1.54178$ Å)
Temperature (°C)	20	20
Transmission factors: max., min.	1.000, 0.578	1.000, 0.623
R[a]	0.046	0.100
R_w[b]	0.070	0.119

[a] $R=\Sigma||F_o|-|F_c||/\Sigma|F_o|$. [b] $R_w=[\Sigma w(|F_o|-|F_c|)^2/\Sigma w|F_o|^2]^{1/2}$; $w=1/\sigma^2(|F_o|)$.

TABLE 2. Positional parameters and B_{eq} for $CpMoCl_3(dmpe)$

Atom	x	y	z	B_{eq}
Mo	0.10771(5)	0.36166(3)	0.84616(2)	1.62(2)
Cl(1)	0.0415(2)	0.3058(1)	0.9923(1)	3.53(7)
Cl(2)	0.3071(2)	0.2204(1)	0.8629(1)	3.29(6)
Cl(3)	−0.1834(2)	0.4288(1)	0.8056(1)	3.83(7)
P(1)	−0.0818(2)	0.2056(1)	0.8129(1)	2.65(6)
P(2)	0.0721(2)	0.3362(1)	0.6785(1)	3.34(7)
C(1)	0.236(1)	0.4861(7)	0.9492(6)	6.6(5)
C(2)	0.141(1)	0.5305(6)	0.8770(8)	5.5(4)
C(3)	0.1940(9)	0.5060(5)	0.7990(5)	4.1(3)
C(4)	0.3313(9)	0.4441(5)	0.8258(5)	4.1(3)
C(5)	0.357(1)	0.4299(6)	0.9195(6)	5.4(4)
C(6)	−0.011(1)	0.0940(5)	0.8711(5)	4.4(3)
C(7)	−0.289(1)	0.2112(7)	0.834(1)	9.5(6)
C(8)	−0.112(2)	0.1744(7)	0.6938(5)	10.7(7)
C(9)	−0.037(2)	0.223(1)	0.6439(6)	13(1)
C(10)	0.258(1)	0.318(1)	0.6337(7)	9.4(7)
C(11)	−0.044(2)	0.425(1)	0.6020(6)	16(1)

TABLE 3. Selected intramolecular distances (Å) and angles (°) for $CpMoCl_3(dmpe)$

Distances (Å)	
Mo–Cl(1)	2.487(1)
Mo–Cl(2)	2.500(1)
Mo–Cl(3)	2.494(2)
Mo–P(1)	2.614(2)
Mo–P(2)	2.481(2)
Mo–C(Cp)[a]	2.30(6)
Angles (°)	
Cl(1)–Mo–Cl(2)	86.69(5)
Cl(1)–Mo–Cl(3)	86.61(6)
Cl(1)–Mo–P(1)	71.36(5)
Cl(1)–Mo–P(2)	147.72(6)
Cl(1)–Mo–Cp[b]	107.5
Cl(2)–Mo–Cl(3)	150.73(5)
Cl(2)–Mo–P(1)	74.71(5)
Cl(2)–Mo–P(2)	85.31(6)
Cl(2)–Mo–Cp[b]	105.1
Cl(3)–Mo–P(1)	76.15(5)
Cl(3)–Mo–P(2)	85.30(6)
Cl(3)–Mo–Cp[b]	104.1
P(1)–Mo–P(2)	76.36(6)
P(1)–Mo–Cp[b]	178.8
P(2)–Mo–Cp[b]	104.8

[a]Average distance. [b]Center of gravity of the cyclopentadienyl ring.

[CpMo(dmpe)$_2$][MoBr$_4$(dppe)]

A single crystal was glued to the inside of a glass capillary which was then sealed under a dinitrogen atmosphere and mounted on the diffractometer. Cell determination, data collection and reduction were carried out in a routine manner. An empirical absorption correction was applied to the data [8a]. Relevant crystal data are assembled in Table 1. The

TABLE 4. Positional parameters and B_{eq} for [CpMo(dmpe)$_2$][MoBr$_4$(dppe)]

Atom	x	y	z	B_{eq}
Mo(1)	0.9583(2)	0.2051(1)	0.2585(2)	3.4(2)
Mo(2)	0.7777(2)	0.5229(2)	0.8082(2)	4.5(2)
Mo(3)	0.7720(3)	0.4609(2)	0.2780(2)	5.2(2)
Mo(4)	1.4718(2)	0.1798(2)	0.1828(2)	5.3(3)
Br(1)	0.8728(3)	0.1361(2)	0.2780(2)	4.8(3)
Br(2)	1.0599(3)	0.2641(2)	0.2360(3)	5.5(3)
Br(3)	0.8575(3)	0.2426(2)	0.1654(3)	6.7(3)
Br(4)	0.9189(3)	0.2485(2)	0.3606(3)	6.0(3)
Br(5)	0.9199(3)	0.5081(2)	0.8003(3)	4.7(3)
Br(6)	0.6405(3)	0.5490(3)	0.8197(3)	8.0(4)
Br(7)	0.7827(3)	0.4707(2)	0.9144(3)	6.4(3)
Br(8)	0.7325(4)	0.4572(2)	0.7206(3)	8.3(4)
P(1)	1.0705(6)	0.1669(4)	0.3351(6)	3.1(6)
P(2)	1.0035(7)	0.1511(4)	0.1724(5)	3.5(6)
P(3)	0.8181(6)	0.5972(5)	0.8760(6)	4.1(7)
P(4)	0.7820(7)	0.5785(5)	0.7071(6)	4.4(7)
P(5)	0.7708(8)	0.4526(5)	0.1536(6)	5.1(8)
P(6)	0.6419(8)	0.4730(5)	0.2266(7)	5.0(7)
P(7)	0.723(1)	0.4139(6)	0.3605(8)	8(1)
P(8)	0.856(1)	0.3942(6)	0.2885(7)	7(1)
P(9)	1.6090(9)	0.2022(6)	0.196(1)	7(1)
P(10)	1.472(1)	0.2589(7)	0.140(1)	10(1)
P(11)	1.366(1)	0.2068(7)	0.240(1)	8(1)
P(12)	1.498(1)	0.1519(6)	0.3009(8)	7(1)
C(1)	1.128(2)	0.136(1)	0.277(2)	3(1)
C(2)	1.069(2)	0.114(2)	0.225(2)	4(1)
C(3)	0.802(2)	0.645(1)	0.813(2)	3(1)
C(4)	0.821(3)	0.633(2)	0.749(2)	6(1)
C(10)	1.053(2)	0.123(2)	0.395(2)	3(1)
C(11)	1.004(2)	0.134(1)	0.445(2)	3(1)
C(12)	0.990(3)	0.101(2)	0.498(2)	6(1)
C(13)	1.022(3)	0.059(2)	0.494(3)	6(1)
C(14)	1.068(3)	0.046(2)	0.448(2)	5(1)
C(15)	1.075(3)	0.078(2)	0.396(2)	5(1)
C(20)	1.143(2)	0.199(2)	0.395(2)	4(1)
C(21)	1.209(3)	0.178(2)	0.427(2)	5(1)
C(22)	1.258(2)	0.204(2)	0.471(2)	4(1)
C(23)	1.247(3)	0.248(2)	0.483(3)	7(2)
C(24)	1.189(3)	0.272(2)	0.455(3)	8(2)
C(25)	1.131(2)	0.248(2)	0.406(2)	4(1)
C(30)	0.932(2)	0.114(1)	0.115(2)	3(1)
C(31)	0.970(3)	0.074(2)	0.088(2)	5(1)
C(32)	0.912(3)	0.043(2)	0.043(3)	8(2)
C(33)	0.835(3)	0.063(2)	0.023(3)	8(2)
C(34)	0.809(3)	0.100(2)	0.050(3)	7(2)
C(35)	0.857(3)	0.127(2)	0.098(2)	5(1)
C(40)	1.057(2)	0.177(2)	0.111(2)	3(1)
C(41)	1.033(3)	0.216(2)	0.072(3)	8(2)
C(42)	1.066(3)	0.231(2)	0.020(3)	6(1)
C(43)	1.128(3)	0.208(2)	0.007(2)	4(1)
C(44)	1.163(3)	0.171(2)	0.036(3)	8(2)
C(45)	1.122(3)	0.154(2)	0.087(3)	6(1)
C(50)	0.770(2)	0.620(2)	0.949(2)	3(1)
C(51)	0.783(3)	0.661(2)	0.968(3)	6(1)
C(52)	0.756(3)	0.682(2)	1.019(3)	7(1)
C(53)	0.714(3)	0.655(2)	1.058(3)	6(1)
C(54)	0.704(3)	0.610(2)	1.038(3)	8(2)

(*continued*)

TABLE 4. (*continued*)

Atom	*x*	*y*	*z*	B_{eq}
C(55)	0.735(3)	0.590(2)	0.978(3)	6(1)
C(60)	0.918(2)	0.603(2)	0.915(2)	3(1)
C(61)	0.946(3)	0.569(2)	0.966(2)	5(1)
C(62)	1.017(3)	0.573(2)	1.000(3)	7(1)
C(63)	1.061(3)	0.609(2)	0.990(2)	5(1)
C(64)	1.034(3)	0.642(2)	0.944(2)	5(1)
C(65)	0.962(3)	0.639(2)	0.909(2)	4(1)
C(70)	0.688(3)	0.601(2)	0.657(2)	4(1)
C(71)	0.686(3)	0.644(2)	0.629(2)	5(1)
C(72)	0.617(3)	0.657(2)	0.591(2)	6(1)
C(73)	0.559(3)	0.628(2)	0.582(2)	5(1)
C(74)	0.560(3)	0.586(2)	0.606(3)	7(2)
C(75)	0.627(3)	0.566(2)	0.651(3)	8(2)
C(80)	0.832(2)	0.568(2)	0.639(2)	4(1)
C(81)	0.842(3)	0.524(2)	0.623(3)	8(2)
C(82)	0.891(3)	0.515(2)	0.570(3)	7(2)
C(83)	0.916(3)	0.551(3)	0.540(3)	8(2)
C(84)	0.911(3)	0.591(2)	0.551(3)	8(2)
C(85)	0.877(3)	0.600(2)	0.601(3)	7(1)
C(90)	0.881(2)	0.507(2)	0.286(2)	4(1)
C(91)	0.813(3)	0.537(2)	0.263(3)	6(1)
C(92)	0.769(3)	0.539(2)	0.318(3)	8(2)
C(93)	0.811(3)	0.514(2)	0.372(3)	7(2)
C(94)	0.876(3)	0.496(2)	0.351(3)	7(1)
C(95)	0.760(3)	0.399(2)	0.104(2)	6(3)
C(96)	0.855(3)	0.477(2)	0.118(3)	10(4)
C(97)	0.689(3)	0.489(2)	0.104(2)	4(1)
C(98)	0.638(2)	0.507(2)	0.147(2)	5(3)
C(99)	0.576(3)	0.426(2)	0.184(3)	10(4)
C(100)	0.575(2)	0.501(2)	0.275(2)	4(1)
C(101)	0.641(4)	0.376(2)	0.330(5)	17(6)
C(102)	0.698(4)	0.443(3)	0.437(3)	15(6)
C(103)	0.797(5)	0.370(3)	0.406(4)	17(7)
C(104)	0.877(3)	0.373(2)	0.377(3)	8(4)
C(105)	0.795(4)	0.339(2)	0.246(3)	11(2)
C(106)	0.934(4)	0.380(3)	0.254(4)	13(2)
C(110)	1.433(3)	0.102(2)	0.161(3)	7(2)
C(111)	1.504(3)	0.113(2)	0.127(3)	8(2)
C(112)	1.473(3)	0.147(2)	0.080(2)	6(1)
C(113)	1.395(4)	0.162(2)	0.080(3)	9(2)
C(114)	1.375(3)	0.132(2)	0.122(3)	8(2)
C(115)	1.665(3)	0.163(2)	0.163(3)	9(2)
C(116)	1.671(3)	0.211(2)	0.283(3)	10(4)
C(117)	1.620(5)	0.253(3)	0.153(5)	16(8)
C(118)	1.563(4)	0.271(4)	0.098(6)	21(9)
C(119)	1.421(3)	0.273(3)	0.056(3)	17(6)
C(120)	1.449(5)	0.312(2)	0.181(4)	16(6)
C(121)	1.369(4)	0.254(2)	0.302(3)	12(5)
C(122)	1.279(3)	0.223(2)	0.181(3)	11(4)
C(123)	1.344(5)	0.158(2)	0.283(4)	13(6)
C(124)	1.400(4)	0.129(2)	0.319(3)	7(4)
C(125)	1.523(4)	0.191(2)	0.380(3)	12(2)
C(126)	1.561(3)	0.105(2)	0.318(2)	9(4)

structure was solved by direct methods, revealing the position of the molybdenum and bromine atoms. Alternate full-matrix least-squares cycles and difference Fourier maps revealed the position of the

TABLE 5. Selected intramolecular distances (Å) and angles (°) for $[CpMo(dmpe)_2][MoBr_4(dppe)]$

Distances (Å)	
Mo(1)–Br(1)	2.575(7)
Mo(1)–Br(2)	2.570(7)
Mo(1)–Br(3)	2.582(6)
Mo(1)–Br(4)	2.565(7)
Mo(1)–P(1)	2.54(1)
Mo(1)–P(2)	2.53(1)
Mo(2)–Br(5)	2.575(7)
Mo(2)–Br(6)	2.581(7)
Mo(2)–Br(7)	2.575(7)
Mo(2)–Br(8)	2.611(8)
Mo(2)–P(3)	2.58(1)
Mo(2)–P(4)	2.58(1)
Mo(3)–P(5)	2.46(1)
Mo(3)–P(6)	2.38(1)
Mo(3)–P(7)	2.39(2)
Mo(3)–P(8)	2.43(2)
Mo(3)–C(90)	2.33(4)
Mo(3)–C(91)	2.36(5)
Mo(3)–C(92)	2.40(6)
Mo(3)–C(93)	2.43(5)
Mo(3)–C(94)	2.37(5)
Mo(4)–P(9)	2.48(2)
Mo(4)–P(10)	2.45(2)
Mo(4)–P(11)	2.46(2)
Mo(4)–P(12)	2.44(2)
Mo(4)–C(110)	2.37(5)
Mo(4)–C(111)	2.35(6)
Mo(4)–C(112)	2.25(5)
Mo(4)–C(113)	2.30(6)
Mo(4)–C(114)	2.38(6)
Angles (°)	
Br(1)–Mo(1)–Br(2)	170.7(3)
Br(1)–Mo(1)–Br(3)	94.7(2)
Br(1)–Mo(1)–Br(4)	91.5(2)
Br(1)–Mo(1)–P(1)	89.5(3)
Br(1)–Mo(1)–P(2)	82.7(3)
Br(2)–Mo(1)–Br(3)	90.9(2)
Br(2)–Mo(1)–Br(4)	95.3(2)
Br(2)–Mo(1)–P(1)	84.0(3)
Br(2)–Mo(1)–P(2)	89.6(3)
Br(3)–Mo(1)–Br(4)	96.2(2)
Br(3)–Mo(1)–P(1)	170.8(4)
Br(3)–Mo(1)–P(2)	92.3(3)
Br(4)–Mo(1)–P(1)	91.8(3)
Br(4)–Mo(1)–P(2)	170.1(3)
P(1)–Mo(1)–P(2)	80.1(4)
Br(5)–Mo(2)–Br(6)	172.3(3)
Br(5)–Mo(2)–Br(7)	92.6(2)
Br(5)–Mo(2)–Br(8)	92.0(2)
Br(5)–Mo(2)–P(3)	88.9(3)
Br(5)–Mo(2)–P(4)	84.7(3)
Br(6)–Mo(2)–Br(7)	90.6(2)
Br(6)–Mo(2)–Br(8)	94.7(3)
Br(6)–Mo(2)–P(3)	83.9(3)
Br(6)–Mo(2)–P(4)	91.7(3)
Br(7)–Mo(2)–Br(8)	94.2(2)
Br(7)–Mo(2)–P(3)	95.7(3)

(*continued*)

TABLE 5. (*continued*)

Br(7)–Mo(2)–P(4)	175.4(3)
Br(8)–Mo(2)–P(3)	169.9(3)
Br(8)–Mo(2)–P(4)	89.5(3)
P(3)–Mo(2)–P(4)	80.6(4)
P(5)–Mo(3)–P(6)	74.8(5)
P(5)–Mo(3)–P(7)	132.6(6)
P(5)–Mo(3)–P(8)	85.0(5)
P(5)–Mo(3)–Cp(9)[a]	112.7
P(6)–Mo(3)–P(7)	87.0(6)
P(6)–Mo(3)–P(8)	133.5(6)
P(6)–Mo(3)–Cp(9)[a]	115.4
P(7)–Mo(3)–P(8)	76.5(6)
P(7)–Mo(3)–Cp(9)[a]	114.6
P(8)–Mo(3)–Cp(9)[a]	111.0
P(9)–Mo(4)–P(10)	74.3(6)
P(9)–Mo(4)–P(11)	132.2(6)
P(9)–Mo(4)–P(12)	87.5(6)
P(9)–Mo(4)–Cp(11)[b]	117.1
P(10)–Mo(4)–P(11)	84.5(7)
P(10)–Mo(4)–P(12)	129.1(7)
P(10)–Mo(4)–Cp(11)[b]	116.7
P(11)–Mo(4)–P(12)	73.4(6)
P(11)–Mo(4)–Cp(11)[b]	111.0
P(12)–Mo(4)–Cp(11)[b]	114.0

[a]Cp(9) = center of gravity of the ring defined by C(90), C(91), C(92), C(93), and C(94). [b]Cp(11) = center of gravity of the ring defined by C(110), C(111), C(112), C(113), and C(114).

other non-hydrogen atoms. Due to the limited amount of data, only the molybdenum, bromine and phosphorus atoms, and the carbon atoms associated with the dmpe ligands were refined anisotropically. Among the dmpe carbon atoms, C(97), C(100), C(105), C(106), C(115) and C(125) refined with a non-positive definite thermal tensor, and were therefore left isotropic. The dmpe related hydrogen atoms were not included. The other hydrogen atoms were included at calculated positions and used for structure factor calculations but not refined. An additional absorption correction was applied at the end of the isotropic refinement according to the method of Walker and Stuart [8b], although this treatment lowered only marginally the agreement factor (from 13.6 to 12.5%). The final agreement factor was 0.10. Positional and equivalent isotropic thermal parameters are assembled in Table 4 and selected bond distances and angles are reported in Table 5.

We identify the following reasons for the relatively high final R factor. The small size of the crystal and its poor diffraction led to observation of only a relatively small fraction of data. In order to keep the observation/parameter ratio to a reasonable value, the $F^2/s\sigma(F^2)$ cutoff limit for observed reflections was 2.5. In addition, the plate-like shape of the crystal and the strong absorption of X-rays, especially with the copper radiation used, made an accurate absorption correction difficult. The highest peaks in the last difference Fourier map (3.34 and 1.70 e $Å^{-1}$) were located at *c.* 1.4 Å from Mo(3) and Mo(4), respectively, i.e. from the Mo centers to which the thermally active dmpe ligands are bonded. There was otherwise no sign of missing atoms or of positional disorder in the structure. All other peaks in the last difference Fourier map had a height <1 e $Å^{-1}$.

Results

Chemical studies

The synthesis of the 17-electron compounds $CpMoX_2(dmpe)$ (X = Cl, Br, I) was attempted by three different routes. The first route consisted of the reduction of $CpMoCl_4$ with two equivalents of sodium in THF, followed by the addition of one equivalent of dmpe, analogous to the synthesis of $CpMoCl_2(dppe)$ [2]. An immediate reaction afforded a precipitate and a solution which exhibited an EPR quintet ($g = 1.999$, $a_p = 24.9$ G or 2.25×10^{-3} cm^{-1}). This quintet decreased in intensity over a few hours and an EPR silent and almost colorless solution was eventually obtained. These observations lead to the following two conclusions. First, two chelating diphosphine ligands (four phosphorus atoms) are equivalently bound to the metal center in the EPR active intermediate. Electron counting excludes a structure with a η^5-Cp ligand *and* the two chloro ligands bound to the metal center. Reasonable possibilities for the structure of this intermediate are $[Mo(\eta^5\text{-Cp})(dmpe)_2]^{2+}(Cl^-)_2$, $[Mo(\eta^3\text{-Cp})Cl(dmpe)_2]^+(Cl^-)$, and $Mo(\eta^1\text{-Cp})Cl_2(dmpe)_2$, each having 17 electrons in the metal valence shell. The first structure is analogous to the compound $[CpMo(dppe)_2][PF_6]_2$ described in the literature [9] (this compound also exhibits an EPR quintet at $g = 1.988$, $a_p = 20.4$ G, in good agreement with our observation). Concerning the other structures, the slippage and eventual replacement of the Cp ring by trialkylphosphine ligands is documented for rhenium [10], molybdenum and tungsten [11], and even for a C_5Me_5 compound of rhodium [12]. Second, since the reaction is carried out with a deficiency of dmpe with respect to the two equivalents suggested by EPR for the intermediate, the $CpMoCl_2(dmpe)$ compound that is presumably formed in the first step must be more reactive toward dmpe than the Mo(III) precursor itself. A subsequent slow reaction takes place, as evidenced by the decrease of the EPR quintet intensity, but the isolated solid is insoluble in all common organic solvents (except for CH_2Cl_2, *vide infra*) and could not be characterized. For the similar reaction between

$[Cp'MoCl_2]_2$ ($Cp' = \eta^5$-C_5H_4-i-Pr) and dmpe reported by Green and coworkers, only compounds with a Mo/dmpe ratio of 1:2, that is $[Cp'Mo(dmpe)_2][PF_6]$ and $[Cp'MoH(dmpe)_2][PF_6]_2$, were isolated and no paramagnetic Mo(III) intermediate was reported [13]. Treatment of the insoluble product with CH_2Cl_2 produced a Mo(IV) material, the known [14] $CpMoCl_3(dmpe)$, in small yields. It is conceivable that the oxidation occurs at the expense of the solvent.

The second route investigated is illustrated in eqns. (1a) and (1b). This strategy successfully yields the analogous dppe products [2] through the intermediate formation of $MoX_3(dppe)(THF)$ [4]. We have not isolated the hypothetical $MoX_3(dmpe)(THF)$ or $[MoX_3(dmpe)]_2$ intermediate, neither of which is described in the literature, but simply added one equivalent of TlCp to the solutions obtained from the interaction of $MoX_3(THF)_3$ and dmpe in THF as solvent after these were complete (as indicated by the dissolution of the sparingly soluble THF adducts).

$$MoX_3(THF)_3 + dmpe \longrightarrow$$

$$'MoX_3(dmpe)(THF)_n' + (3-n)THF \quad (1a)$$

$$'MoX_3(dmpe)(THF)_n' + TlCp \longrightarrow$$

$$CpMoX_2(dmpe) + TlX + nTHF \quad (1b)$$

4

Reaction (1b) is fast at room temperature. An EPR analysis of the solutions carried out promptly after the addition of TlCp does reveal the presence of the mononuclear $CpMoX_2(dmpe)$ compounds (see Fig. 1). However, a solid promptly precipitates out of these solutions concomitantly with the decrease of the EPR signals, and an EPR silent solution is eventually obtained. The solid product is only sparingly soluble in organic solvents and separation from the thallium by-products proved impossible. The EPR spectra shown in Fig. 1 are very similar to those obtained for the corresponding dppe compounds [2]. The triplet which is clearly observed for X = Cl indicates that two equivalent phosphorus atoms are bound to the metal center. On going from X = Cl to Br to I, the EPR lines broaden while the g value increases. These effects were also observed for the dppe analogues [2]. The g values for the dmpe and dppe compounds with the same halide ligand are almost identical, indicating that this parameter is not very sensitive to the nature of the phosphine.

The third and final route that we have investigated consists of ligand exchange from the $CpMoX_2(dppe)$ products (eqn.(2)). The latter compounds were prepared *in situ* from $MoX_3(dppe)(THF)$ and TlCp as described previously [2], and dmpe was added after filtration of the TlX products. Paralleling the pathway

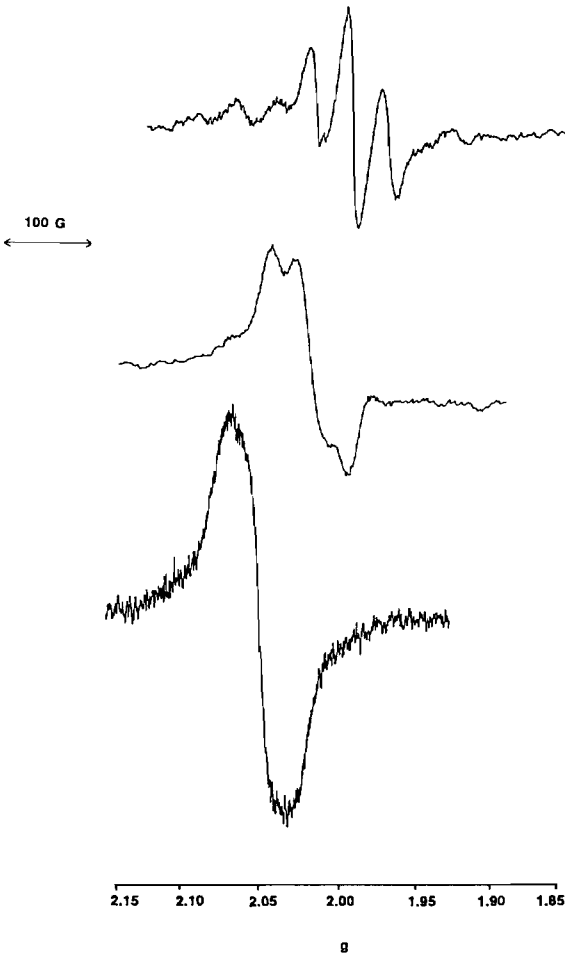

Fig. 1. EPR spectra of solutions obtained by the interaction of $MoX_3(THF)_3$ with dmpe, followed by treatment with TlCp. Solvent: THF; room temperature.

of the second synthetic strategy (eqn. (1b)), insoluble solids precipitated promptly after addition of dmpe. Characterization of these solids has been unsuccessful, even though through this synthetic route there is no contamination by a thallium salt. Elemental analyses and IR spectra indicated that they probably are mixtures of different compounds.

$$CpMoX_2(dppe) + dmpe \longrightarrow$$

$$CpMoX_2(dmpe) + dppe \quad (2)$$

For the case of X = Br, crystals suitable for an X-ray investigation were slowly obtained from the mother solution upon standing at room temperature. X-ray analysis and other pertinent characterization (*vide infra*) established their nature as the salt $[CpMo(dmpe)_2][MoBr_4(dppe)]$.

Structural studies

$CpMoCl_3(dmpe)$

Although this compound had been reported earlier [14], its molecular structure had not been established. The structure of $CpMoCl_3(dmpe)$, which is illustrated in Fig. 2, is analogous to the structure of the related dppe complex reported by Stärker and Curtis [15], and can be described as pseudo-octahedral if the Cp ligand is regarded as occupying one coordination position. The meridional arrangement of the chloride ligands is maintained in solution as indicated by ^1H and ^{31}P NMR, which show two inequivalent PMe_2 moieties. With respect to $CpMoCl_3(dppe)$ [15], the dmpe structure shows the following features: the Mo–Cl distances are on average 0.02 Å longer, the Mo–P distances are shorter (0.07 Å for the axial, i.e. *trans* to Cp, phosphorus atom, and 0.04 Å for the equatorial one), and the average Mo–C(Cp) distance is *c.* 0.02 Å shorter. These variations are probably the direct or indirect result of the better σ-donor ability of dmpe.

$[CpMo(dmpe)_2][MoBr_4(dppe)]$

The compound crystallizes with two independent cations and two independent anions in the asymmetric unit, with both pairs of ions displaying very similar structural parameters. Although the relatively poor quality of the data (see 'Experimental') does not allow detailed comparisons to be made, the minor differences are probably due to packing forces. Views of the cation and anion are shown in Figs. 3 and 4, respectively. The $[CpMo(dmpe)_2]^+$ cation exhibits a typical four-legged piano-stool geometry as found in many other monocyclopentadienyl derivatives of Mo(II). The geometry at the four legs is distorted by the requirements of the chelating diphosphines, the bite angles of the dmpe ligands averaging 75(1)°, whereas the *cis* angles between different dmpe ligands average 86(1)°. The Mo–P distances in the two cations average 2.42(4) and 2.46(2) Å, respectively.

The $[MoBr_4(dppe)]^-$ anion has a pseudo-octahedral coordination of the ligands. A different salt of the same anion has been crystallographically characterized earlier [17]. The bond distances in the two

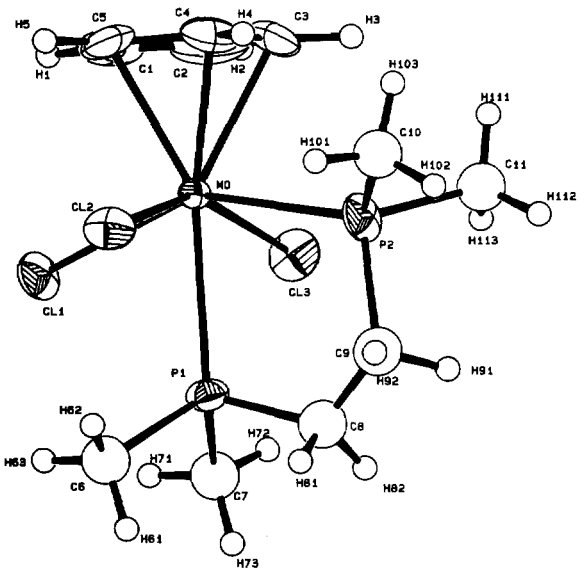

Fig. 2. An ORTEP view of the $CpMoCl_3(dmpe)$ molecule. Hydrogen atoms are drawn with arbitrary radii for clarity. Atoms C(6)–C(11) are also drawn with arbitrary radii. The plot file was modified with the program PLOTMD for label position optimization [16].

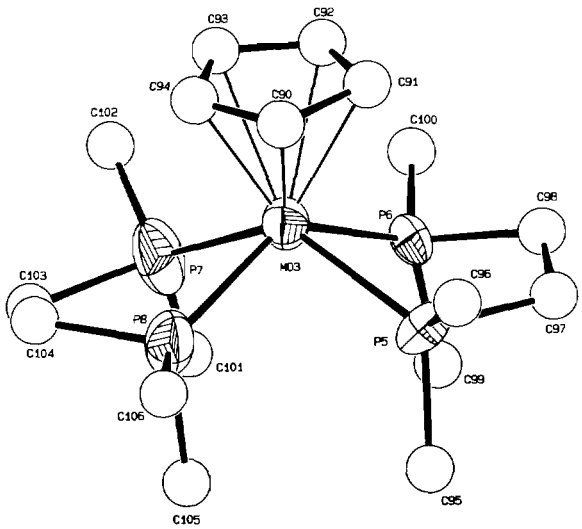

Fig. 3. An ORTEP view of the $[CpMo(dmpe)_2]^+$ cation with the numbering scheme employed. The plot file was modified with the program PLOTMD for label position optimization [16].

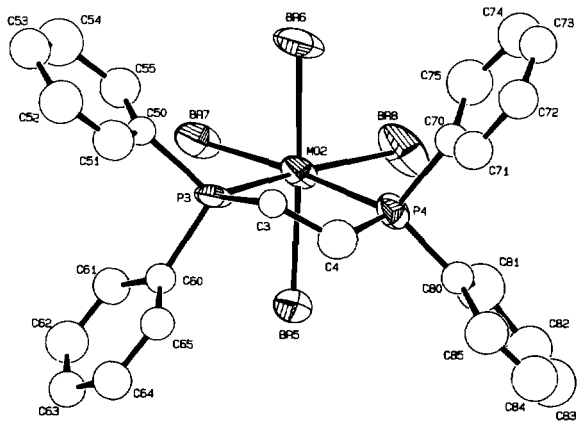

Fig. 4. An ORTEP view of the $[MoBr_4(dppe)]^-$ anion with the numbering scheme employed. The plot file was modified with the program PLOTMD for label position optimization [16].

different salts compare well (Mo–Br: 2.573(7) and 2.58(2) Å for the two independent molecules in the $[CpMo(dmpe)_2]^+$ salt, 2.58(1) Å for the NBu_4^+ salt; Mo–P: 2.54(1) and 2.58(1) Å for our compound, 2.532(8) Å for the NBu_4^+ salt).

Discussion

The reactions that led to the formation of the title compounds are described in 'Results'. The formation of Mo(IV) material by treatment of the insoluble Mo(III) product and CH_2Cl_2 is consistent with the low potential required for the one-electron oxidation of materials of $CpMoCl_2L_2$ (L = phosphine) stoichiometry [1, 2].

Concerning the $[CpMo(dmpe)_2][MoBr_4(dppe)]$ material, a total of five negatively charged ligands (one Cp^- and four Br^-) are present among the two ions, establishing a total charge of 5+ for the two molybdenum centers. The only reasonable oxidation number assignments are +2/+3 and +3/+2. The +1/+4 and +4/+1 possibilities are not considered as they would lead to an unreasonable electron count for at least one of the two ions. In addition, the former possibility (+1/+4) would correspond to uncharged species, which seems unreasonable (although not impossible) since the two molecules co-crystallize in a 1:1 ratio. For similar reasons we do not consider the 0/+5 assignments.

The structural data favor the formulation of the compound as containing a Mo(II) monocation and a Mo(III) monoanion. In particular, the bond distances in the $[MoBr_4(dppe)]^-$ ion are in good agreement with those observed for the same ion in the NBu_4^+ salt [17]. The alternative +3/+2 formulation would lead to doubly charged ions. There is no existing example of salts containing the Mo(II) $[MoX_4L_2]^{2-}$ ions (X = negatively charged ligand; L = neutral monodentate ligand, or L_2 = neutral bidentate ligand) [18], whereas there are many examples of Mo(III) $[MoX_4L_2]^-$ monoanions, including the $[MoBr_4(dppe)]^-$ ion [17]. However, both the $[CpMo(diphosphine)_2]^{n+}$ cations of Mo(II) ($n=1$) and Mo(III) ($n=2$), are known for the diphosphine dppe [9].

Additional evidence (although negative) is obtained by EPR for the assignment of the +II oxidation state to the Mo center in the cation. The Mo(II) $[CpMo(dmpe)_2]^+$ cation is an 18-electron, diamagnetic species, expected to display no EPR signal. On the other hand, the hypothetical $[CpMo(dmpe)_2]^{2+}$ species is a paramagnetic, 17-electron complex which is anticipated to exhibit a sharp room temperature EPR spectrum, as seen for the isolated dppe-containing analogue, $[CpMo(dppe)_2]^{2+}$ [9]. As far as the anion is concerned, neither the $[MoBr_4(dppe)]^{2-}$ ion of Mo(II) (d^2), nor the $[MoBr_4(dppe)]^-$ ion of Mo(III) (d^3) are expected to show room temperature EPR signals, the latter because of the fast spin relaxation associated with the high spin configuration ($S=3/2$) [19]. Methylene chloride solutions of $[CpMo(dmpe)_2][MoBr_4(dppe)]$ are observed to be EPR silent at room temperature. Also, Green and coworkers have isolated $[Cp'Mo(dmpe)_2]PF_6$, which contains an analogous Mo(II) cation, by interaction of $[Cp'MoCl_2]_2$ ($Cp' = \eta^5$-C_5H_4-i-Pr) and dmpe [13].

We do not know the reason for the different chemical behavior of $CpMoX_2$(L-L) derivatives when L-L = dmpe or dppe. The dppe derivatives are stable in solution and in the solid state [2] whereas the dmpe compounds (which, as we have shown above, can be generated as transient species) rapidly decompose to insoluble products. The instability of the dmpe adducts is striking especially when considering that the derivatives with monodentate phosphine ligands $CpMoX_2L_2$ ($L=PMe_3$ [1], PPh_3 [20]) are equally stable. Unfortunately, the nature of the main product(s) of the dmpe reactions could not be clarified.

Supplementary material

Full tables of bond distances and angles, anisotropic displacement parameters, hydrogen atom positions, and F_o/F_c data for compounds $CpMoCl_3$(dmpe) and $[CpMo(dmpe)_2][MoBr_4(dppe)]$ are available from the senior author upon request.

Acknowledgements

We are grateful to the University of Maryland, College Park, (UMCP) Department of Chemistry and Biochemistry, the UMCP General Research Board, the Camille and Henry Dreyfus Foundation (through a Distinguished New Faculty Award to R. P.) and the Donors of the Petroleum Research Fund, administered by the American Chemical Society, for support. The X-ray diffractometer and Micro Vax computer system were purchased in part with NSF funds (CHE-84-02155).

References

1 S. T. Krueger, R. Poli, A. L. Rheingold and D. L. Staley, *Inorg. Chem.*, *28* (1989) 4599.
2 S. T. Krueger, B. E. Owens and R. Poli, *Inorg. Chem.*, *29* (1990) 2001.

3 (a) B. E. Owens and R. Poli, *198th National ACS Meet., Miami Beach, FL, Sept. 10–15, 1989,* Comm. INOR 123; (b) R. G. Linck, B. E. Owens and R. Poli, *200th National ACS Meeting, Washington, DC, Aug. 26–31 (1990),* Comm. INOR 38.

4 J. R. Dilworth and R. L. Richards, *Inorg. Synth., 20* (1980) 121.

5 B. E. Owens, R. Poli and A. L. Rheingold, *Inorg. Chem., 28* (1989) 1456.

6 F. A. Cotton and R. Poli, *Inorg. Chem., 26* (1987) 1514.

7 R. Poli and A. L. Rheingold, *J. Chem. Soc., Chem. Commun.,* (1990) 552.

8 (a) A. C. T. North, D. C. Phillips and F. S. Mathews, *Acta Crystallogr., Sect. A, 24* (1968) 351; (b) N. Walker and D. Stuart, *Acta Crystallogr., Sect. A, 39* (1983) 158.

9 J. A. Segal, M. L. H. Green, J.-C. Daran and K. Prout, *J. Chem. Soc., Chem. Commun.,* (1976) 766.

10 (a) C. P. Casey, J. M. O'Connor and K. J. Haller, *J. Am. Chem. Soc., 107* (1985) 3172. (b) J. M. O'Connor and C. P. Casey, *Chem. Rev., 87* (1987) 307.

11 N. J. Christensen, A. D. Hunter, P. Legzdins and L. Sanchez, *Inorg. Chem., 26* (1987) 3344.

12 M. Paneque and P. M. Maitlis, *J. Chem. Soc., Chem. Commun.,* (1989) 105.

13 P. D. Grebenik, M. L. H. Green, A. Izquierdo, V. S. B. Mtetwa and K. Prout, *J. Chem. Soc., Dalton Trans.,* (1987) 9.

14 G. S. B. Adams and M. L. H. Green, *J. Chem. Soc., Dalton Trans.,* (1981) 353.

15 K. Stärker and M. D. Curtis, *Inorg. Chem., 24* (1985) 3006.

16 J. Luo, H. Ammon and G. L. Gilliland, *J. Appl. Crystallogr., 22,* 186 (1989).

17 P. Salagre, J.-E. Sueiras, X. Solans and G. Germain, *J. Chem. Soc., Dalton Trans.,* (1985) 2263.

18 (a) F. A. Cotton and G. Wilkinson, *Advanced Inorganic Chemistry;* Wiley, New York, 5th edn., 1988; (b) G. Wilkinson, R. D. Gillard and J. A. McCleverty (eds.), *Comprehensive Coordination Chemistry,* Pergamon, Oxford, 1987.

19 (a) H. S. Jarrett, *J. Chem. Phys., 27* (1957) 1298; (b) P. C. H. Mitchell and R. D. Scarle, *J. Chem. Soc., Dalton Trans.,* (1975) 110; (c) B. A. Averill and W. H. Orme-Johnson, *Inorg. Chem., 19* (1980) 1702; (d) M. Millar, S. H. C. J. Lincoln and S. A. Koch, *J. Am. Chem. Soc., 104* (1982) 288.

20 R. Poli and B. E. Owens, to be published.